

*Letter to the Editor***A calibration of the ROSAT HRI UV leak**T.W. Berghöfer^{1,2}, J.H.M.M. Schmitt¹, and M. Hünsch³¹ Hamburger Sternwarte, Universität Hamburg, Gojenbergsweg 112, D-21029 Hamburg, Germany² Space Sciences Laboratory, University of California, Berkeley, CA 94720, USA³ Institut für Theoretische Physik und Astrophysik der Universität Kiel, Olshausenstrasse 40, D-24118 Kiel, Germany

Received 16 November 1998 / Accepted 24 November 1998

Abstract. The purpose of this paper is to present a detailed investigation of the Ultraviolet and visible sensitivity of the high-resolution imager (HRI) onboard the ROSAT X-ray satellite. We provide observational evidence that a recently published model (Zombeck et al. 1997) of the out-of-band quantum efficiency of the HRI overpredicts the detector response longward of approximately 4000Å. The contamination of the HRI is limited to the UV bandpass below approximately 4000Å. Based on the optical properties of our target stars, our ROSAT HRI and PSPC observations, and UV fluxes measured with the TD1 satellite, we provide an accurate calibration for the UV leak flux and present formulae to estimate UV leak count rates based on UV (1965Å) fluxes or stellar U magnitudes.

Key words: instrumentation: detectors – stars: early-type – X-rays: stars

1. Introduction

X-ray surveys have shown ubiquitous X-ray emission from stars over almost the entire HR diagram. The early-type stars are known to be X-ray emitters as well as late-type stars later than A7. For a detailed discussion of the X-ray emission of early-type stars, which is generally assumed to be produced in the stellar winds, we refer to Berghöfer et al. (1997) and references therein. Following Berghöfer et al. (1997), early-type stars to the right of the hot star X-ray dividing line at spectral type B1 should be devoid of any significant intrinsic X-ray emission. Late-type stellar X-ray emission originating from hot coronae starts at spectral type A7 (Schmitt et al. 1985, Schmitt 1997). Therefore, X-ray detected stars of spectral types B2 – A6 are generally believed to have X-ray emitting late-type companions and the observed emission is generally thought not to be intrinsically related to the B or A star itself; the X-ray detection rate for B2 – A6 stars is $\approx 10\%$ (Berghöfer et al. 1997, Berghöfer et al. 1998). For a discussion of X-ray detected early-type stars of these spectral types we refer to Berghöfer & Schmitt (1994) and Berghöfer et al. (1998).

Send offprint requests to: T.W. Berghöfer

Many early-type stars have been observed with the ROSAT high-resolution imager (HRI) or have been serendipitously detected. A detailed description of the HRI can be found in Zombeck et al. (1995), whereas a general overview of the ROSAT project is provided by Trümper (1983) and Trümper et al. (1991). The HRI detector is known to show a response to ultraviolet and/or optical radiation (Schmitt et al. 1993, Zombeck et al. 1997). For objects apparently bright at UV wavelengths but X-ray faint or X-ray dark (e.g., early-type stars), the contamination of the X-ray data resulting from the HRI UV leak can significantly contribute to the overall HRI count rate.

The HRI consists of a configuration of two microchannel plates (MCPs) in front of an electronic readout. In order to improve the quantum efficiency of the HRI at soft X-ray energies the front plate is coated with cesium iodide which also results in a higher response to radiation at wavelengths above 1100Å. Additionally, the HRI is equipped with an UV/ion shield which consists of a polypropylene/aluminum and Lexan/aluminum filter pair to reduce the effect of UV contamination.

In principle, the design of the HRI detector allows a discrimination of 16 pulse height channels. The bulk portion of the UV/optical contamination appears in the HRI detector channels 1–3. Thus, an exclusion of channels 1–3 can eliminate the bulk portion of the contaminating flux. However, the spectral response of the HRI is very poor; according to Preston et al. (1998), the HRI pulse height distribution can be used to compute a 2 band hardness ratio under certain limitations. The HRI detector channels 1–3 therefore show a combination of true X-ray flux and contamination from wavelengths above 1100Å. An exclusion of channels 1–3 obviously leads to a loss in total count rate.

Zombeck et al. (1997) investigated the UV and optical response of the HRI detector by means of laboratory transmission measurements of flight back-up UV/Ion shield components. These authors show that optical interference within one filter (aluminized Lexan) of the pair comprising the UV/Ion shield leads to a much larger shield transmission at UV and visible wavelengths than previously inferred from model calculations of the individual filters. Based on their transmission measurements and estimates of the UV quantum efficiency of the HRI

Table 1. Observation log of calibration target

star	SP.	U	B	V	TD1		HRI			PSPC		
					flux(1965Å) (10^{-9} erg cm $^{-2}$ s $^{-1}$ Å $^{-1}$)	flux(2740Å)	ROR	rate	σ	ROR	rate	σ
Rigel	B8Iab	-0.57	0.09	0.12	8.012	6.024	202520h	0.1960	0.0096	200115p	<0.0015	
Betelgeuse	M1-2Ia	4.41	2.35	0.5	$4 \cdot 10^{-4}$	0.016	202250h	<0.0005		survey	<0.012	
β Aur	A2IV	1.98	1.93	1.85	0.618	0.413	141847h	0.0078	0.0019	141852p	<0.002	
HR 2844	B9Mnp	5.21	5.62	5.72	0.069	0.035	201634h	<0.0018		survey	<0.011	
β Car	A2IV	1.65	1.68	1.70	0.755	0.500	100603h	0.0111	0.0010	100359p	<0.0004	
Vega	A0V	0.02	0.03	0.03	4.928	3.123	141905h	0.0937	0.0035	160085p	<0.001	
ζ Aql	A0V	2.99	3.00	2.99	0.287	0.193	201651h	<0.0042		survey	<0.014	

MCPs, Zombeck et al. (1997) modelled the effective area of the HRI in the wavelength range 1200–6000Å. The UV quantum efficiency of CsI-coated MCPs at UV and optical wavelength has been measured by Martin & Bowyer (1982). However, no measurements exist in the wavelength range 2537–5500Å. Zombeck et al. (1997) interpolated this wavelength range by two different functions, an exponential function plus constant value and a logarithmic function. According to their Fig. 2, the latter seems to provide an upper limit for the quantum efficiency in this wavelength range, whereas the exponential function plus constant value provides a lower limit.

Zombeck et al. (1997) then folded the UV and optical spectrum of the optically bright A0V stars Vega and β Car with the two model effective areas, resulting from the combined UV shield transmission, MCP quantum efficiency (two models) and effective area of the ROSAT mirror assembly, respectively, to predict contamination count rates for the UV and optical leak of the HRI. Both stars do not show any X-ray emission during longer pointings with the ROSAT PSPC and hence confirm that the UV quantum efficiency of the PSPC is low. The results derived by Zombeck et al. (1997) indicate that a large fraction of the contamination might be related to contamination from light longward of 2000Å and that extending to 6000Å and that the effect of a possible leak in the 1500–1700Å band leak is minor. The two different interpolations of the MCP quantum efficiency result in different count rate predictions in the wavelength band 2500–6000Å. The count rates obtained for the higher quantum efficiency seem to be consistent with the observations, whereas the lower quantum efficiency at optical wavelengths leads to significantly lower count rates than observed. However, these authors also point out that their laboratory measurements cannot reliably predict the detector response in the wavelength range 2500–5500Å and a calibration of the HRI effective area in the UV and optical range can only be done with observations of UV and/or optically bright sources.

The purpose of this paper is to present such a calibration for the HRI UV leak flux which allows to determine the amount of UV contamination to the HRI count rate of celestial sources with known UV and optical fluxes.

Our investigation involves ROSAT HRI and PSPC data of selected B and A stars obtained during the ROSAT pointing pro-

gram. For stars not observed during the PSPC pointing program we included the ROSAT all-sky survey (RASS) count rates or upper limits. First, we describe our target selection, all data material, and the data reduction. Second, we compare the observed HRI count rates with the stellar optical brightnesses and UV fluxes measured with the TD1 satellite (Thompson et al. 1978) and present the results of our investigation. Third, we discuss our results in the context of earlier studies and derive our conclusions.

2. Calibration targets and data analysis

For our investigation of the UV response of the ROSAT HRI we selected optically bright late B and early A stars observed with the HRI and without any detectable flux during observations with the PSPC. We assume that these stars do not produce any intrinsic X-ray emission which is justified by the fact of a low PSPC count rate or upper limit. Note that the late B supergiant Rigel (β Ori) is listed in the ROSAT all-sky survey OB star catalog (Berghöfer et al. 1996) with a PSPC count rate of 0.027 ± 0.011 cts s $^{-1}$. A later 6 ksec observation with the PSPC centered on β Ori showed that the X-ray emission observed during the moderately resolved RASS is associated with a nearby late-type star located at an angular distance of 43'' to the primary. Based on this observation we derived an upper limit PSPC count rate of 0.0015 cts s $^{-1}$ for the late B supergiant β Ori.

The selected late B and A stars are all optically and UV bright sources. In order to test whether the contamination of the HRI is caused only by UV radiation, or only optical radiation, or both, we included a recent observation of the late-type supergiant Betelgeuse (α Ori). This star is optically bright but very red ($B-V=1.85$) and does not show any significant UV flux or X-ray emission.

In Table 1 we provide observational data of our calibration stars: the star's name, its spectral type, U, B, and V magnitudes, the UV fluxes at 1965Å and 2740Å measured with TD1, and the ROSAT observation number (ROR), count rate and count rate error of the respective HRI and PSPC observations. The stellar parameters have been taken from the Bright Star Catalog (Hoffleit & Warren 1991) and the UV fluxes are taken from the catalog of stellar UV fluxes (Thompson et al. 1978)

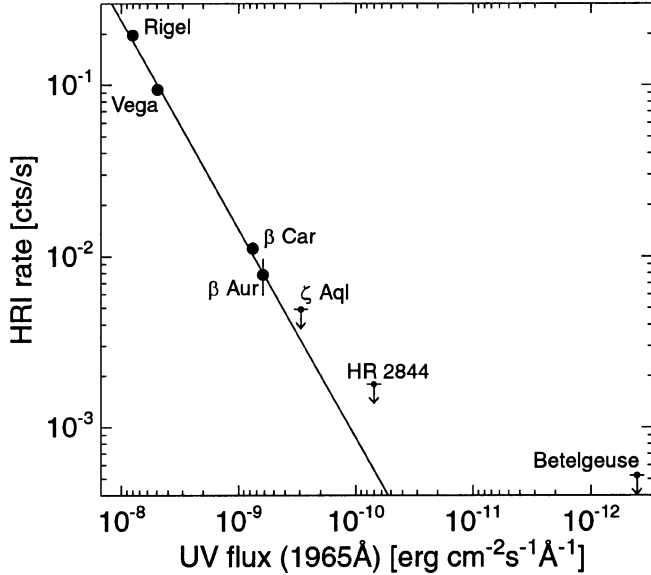


Fig. 1. HRI count rates plotted vs. UV fluxes at 1965Å.

The ROSAT observations of our calibration targets have been reduced with the EXSAS software (Zimmermann et al. 1994), which is based on the ESO MIDAS software package. We used standard procedures to derive the background corrected count rates in the HRI detector pulse height channels 1–8 for our calibration targets. These channels have been selected in order to improve the signal-to-noise ratio. For X-ray sources observed in the center of the HRI field of view the other pulse height channels are dominated by noise and do not contribute to the X-ray signal. The UV leak contamination is also expected to predominantly appear in channels 1–3. Note that all our targets were observed in the detector center. Therefore, the discrimination of pulse height channels 0 and 9–15 should not cause any loss in flux which has been reported for pulse height channel selections of HRI sources observed at larger off-axis angles. A visual inspection of the pulse height distributions of our calibration targets showed that the actual signal is present only in channels 1–8, and the bulk portion is concentrated to channels 1–3 indicative of UV contamination.

2.1. The UV calibration of the HRI

For our sample of calibration stars we now compare the observed HRI count rates with the stellar UV fluxes and optical brightnesses. In Fig. 1 we plot the HRI count rates as a function of the TD1 UV fluxes at 1965Å. As can be seen the HRI count rates are well correlated with the stellar UV fluxes at 1965Å. The upper limit of the red supergiant Betelgeuse is consistent with the regression curve derived from A-type stars. In order to derive the relation between the HRI count rates and UV fluxes we performed a linear regression analysis. The formal result is

$$\text{HRI}_{UV} = (-0.0088 \pm 0.024) + (2.42 \pm 0.13) \times 10^7 \cdot \frac{f(1965\text{\AA})}{[\text{erg cm}^{-2}\text{s}^{-1}\text{\AA}^{-1}]} \quad [\text{cts s}^{-1}] \quad (1)$$

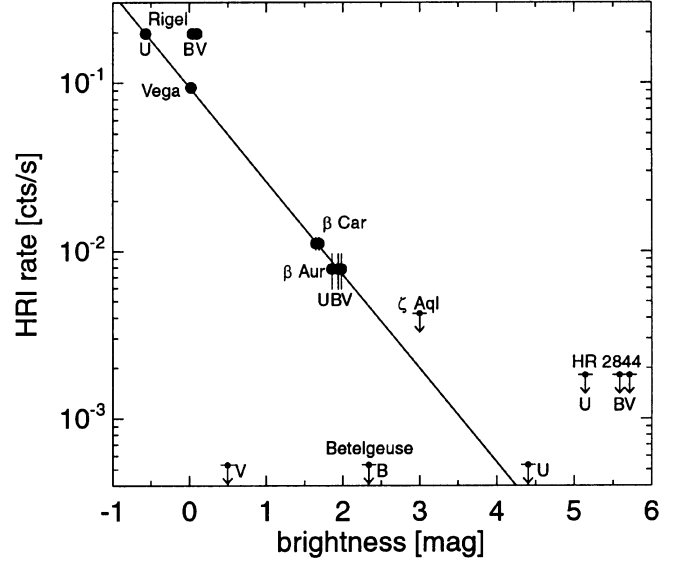


Fig. 2. HRI count rates plotted vs. stellar UB magnitudes. The solid line shows the results of a regression analysis of the HRI count rates as a function of stellar U magnitudes for the stars Rigel, Vega, β Car and β Aur.

The formal result of our regression analysis is and is shown as a solid line in Fig. 1.

A plot of the HRI count rates versus the stellar TD1 fluxes at 2740Å shows this tight correlation as well, only the Betelgeuse upper limit appears closer to the best fit line but is still not sensitive.

In Fig. 2 we show a plot of the HRI count rates as a function of the stellar U, B, and V magnitudes; note that for Vega and β Car these magnitudes are almost identical. The HRI count rates of Rigel, Vega, β Car and β Aur are well correlated with U magnitudes; the U band peaks near 3500Å. The results of a regression analysis for these 4 stars are

$$\text{HRI}_{UV} = 10^{(-1.022 \pm 0.003) - (0.555 \pm 0.005) \cdot U} \quad [\text{cts s}^{-1}], \quad (2)$$

The Betelgeuse observation is consistent with the correlation between stellar U magnitudes and HRI leak count rate.

As can be seen from Fig. 2 the B8Iab star Rigel significantly deviates from the correlations with stellar B and V magnitudes derived for the A stars Vega, β Car and β Aur. Rigel is the hottest star in our sample of calibration stars and the different spectral flux distribution in the optical can account for that. Very importantly, the red supergiant Betelgeuse is much brighter in the B and V bands than in the U band. If significant flux in the B and V band were to contribute to the observed HRI count rate for Vega and β Car, similar values should be encountered for Betelgeuse. This is not observed and we therefore conclude, that flux in the B and V band does not significantly contribute to the observed HRI contamination.

2.2. Discussion and conclusions

Based on ROSAT observations of selected early-type stars and the red supergiant star Betelgeuse we have explored the response

of the HRI detector to UV and optical radiation. We confirm that the contamination is mainly concentrated to pulse height channels 1–3. The contamination count rate is well correlated with the early-type star's apparent UV fluxes at 1965Å and 2740Å and the stellar U magnitudes. Eq. 1 and 2 provide formulae for the HRI leak count rate as functions of stellar UV flux at 1965Å or stellar U magnitudes. These formulae can be used to determine the amount of contamination to an observed HRI count rate of an UV and/or optically bright celestial source observed with the ROSAT HRI.

We now turn to the question whether optical radiation significantly contributes to the overall contamination of the HRI count rates. Our investigations show (cf. Fig. 2) that the HRI detector response should be low at wavelengths above 4000Å.

Zombeck et al. (1997) predict HRI count rates due to contamination in the wavelength range 1100–6000Å for the stars Vega and β Car. Their logarithmic interpolation of the MCP quantum efficiency between 2500–6000Å leads to count rates that explain the observed values for the stars Vega and β Car. In order to test whether or not the HRI upper limit obtained for the red supergiant Betelgeuse can be explained by one of the total effective areas provided by Zombeck et al. (1997), we determined the predicted HRI contamination count rates by folding the optical/UV spectrum of Betelgeuse with the two different effective areas. Based on the logarithmic interpolation of the MCP quantum efficiency between 2500–6000Å we predict a count rate of 0.0087 counts/s, whereas the exponential interpolation leads to a count rate of 0.00044 counts/s. The fact that Betelgeuse was not detected during the 11.5 ksec observation shows that the model for the effective area based on the logarithmic interpolation of the MCP must overestimate the visible light contamination of the HRI detector. Therefore, the detector quantum efficiency at UV wavelengths must be higher than given by Zombeck et al. (1997) to explain the HRI count rates of the observed early-type stars and the upper limit of the red supergiant Betelgeuse.

In summary, our investigations show that the HRI UV contamination is explained by UV radiation only, possibly extending to wavelengths up to 4000Å. Additional laboratory measurements are needed to further investigate the quantum efficiency of the ROSAT HRI.

Acknowledgements. The ROSAT project has been supported by the Bundesministerium für Bildung, Wissenschaft, Forschung und Technologie (BMBF) and the Max-Planck-Gesellschaft (MPG). T.W.B. acknowledges the support from the Alexander-von-Humboldt-Stiftung (AvH) by a Feodor-Lynen Fellowship.

References

- Berghöfer T.W., Schmitt J.H.M.M., 1994, *A&A* 292, L5
 Berghöfer T.W., Schmitt J.H.M.M., Cassinelli J.P., 1996, *A&AS* 118, 481
 Berghöfer T.W., Schmitt J.H.M.M., Danner R., Cassinelli J.P., 1997, *A&A* 322, 167
 Berghöfer T.W., Schmitt J.H.M.M., Rosso, C., 1998, *A&A*, in prep.
 Hoffleit D.E., Warren W.H. Jr., *The Bright Star Catalog*, 5th Rev. Ed., 1991, Yale University Observatory, New Haven CT
 Martin C., Bowyer S., 1982, *Appl. Opt.* 21, 4206
 Pfeffermann E., Briel U., Hippmann H., et al., 1986, *Proc. SPIE* 733, 519
 Preston A.H., Silverman J., McDowell J., et al., 1998, Spectral calibration of the ROSAT HRI, ROSAT science data center at SAO, Harvard
 Schmitt J.H.M.M., Golub L., Harnden F.R. Jr., Maxson C.W., Rosner R., Vaiana G.S. 1985, *ApJ*, 290, 307
 Schmitt J.H.M.M., Zinnecker H., Cruddace R., Harnden F.R. Jr., 1993, *ApJ* 402, L13
 Schmitt J.H.M.M. 1997, *A&A*, 318, 215
 Thompson G.I., Nandy, K., Jamar, C., et al., 1978, The catalogue of stellar ultraviolet fluxes (TD1): A compilation of absolute stellar fluxes measured by the Sky Survey Telescope (S2/68) aboard the ESRO satellite TD-1, The Science Research Council, U.K.
 Trümper J., 1983, *Adv. Space Res.* Vol. 2, No. 4, 241
 Trümper J., Hasinger G., Aschenbach B., et al., 1991, *Nature* 349, 579
 Zimmermann U., et al., 1994, *EXSAS User's Guide*, MPE-Report 257
 Zombeck M.V., David, L., Harnden, F. R., Kearns, K., 1995, *Proc. SPIE* 2518, 304
 Zombeck M.V., Barbera, M., Collura, A., & Murray, S. S., 1997, *ApJ* 487, L69